Rotational Spectrum of the Dimethyl Ether−Acetylene Complex: Evidence for an Effective C_{2v} Geometry

Josh J. Newby, Michal M. Serafin, Rebecca A. Peebles, and Sean A. Peebles*

Department of Chemistry, Eastern Illinois University, 600 Lincoln Avenue, Charleston, Illinois 61920

Received: February 11, 2005; In Final Form: April 26, 2005

The rotational spectra for five isotopomers of the 1:1 weakly bound complex formed between dimethyl ether (DME) and acetylene (HCCH) have been measured by Fourier transform microwave spectroscopy. The experimental rotational constants, planar moments, and dipole moment components are consistent with a floppy complex possessing an effective C_{2v} structure in which the hydrogen atom of acetylene is hydrogen bonded to the oxygen atom of dimethyl ether with an intermolecular H···O separation of 2.08(3) Å. Experimental rotational constants for the normal isotopic species are $A = 10382.5(17)$ MHz, $B = 1535.7187(18)$ MHz, and $C = 1328.3990(17)$ MHz and the dipole moment components are $\mu_a = \mu_{\text{total}} = 1.91(10)$ D. Ab initio calculations at the MP2/6-311++G(2d,2p) level indicate that the energy barrier for motion of the HCCH subunit between the lone pairs of the DME, via a C_{2v} intermediate structure, is very low (~0.29 kJ mol^{-1}). Inclusion of basis set superposition error and zero point energy corrections to the energies of four stationary points located on the potential energy surface shows that the relative stabilities are particularly sensitive to these corrections. The ab initio optimizations give rotational constants for the C_{2v} structure of $A = 10066$ MHz, $B = 1496$ MHz, and $C = 1324$ MHz, and a dipole moment of $\mu_a = \mu_{\text{total}} = 2.12$ D, in reasonable agreement with the experimentally determined values. The structural parameters and energetics of the DME−HCCH complex will be discussed and compared to similar complexes such as H_2O−HCCH.

I. Introduction

Recent high-resolution rotational studies of complexes of dimethyl ether (DME) with proton donors such as HF[1] and HCl[2] have revealed that the HX molecule coordinates to a lone pair of the DME. A tunneling motion of the HX between the two lone pairs of the ether causes significant inversion splittings in the rotational spectrum. Analysis of these splittings led to experimental inversion barriers of 0.71 and 0.83 kJ mol^{-1} for DME−HF[1] and DME−HCl,[2] respectively. It seems reasonable therefore to predict that a similar structure to the HF and HCl complexes, in which the relatively acidic proton of the HCCH interacts with the O atom of the DME, would be observed for DME−HCCH.

In a microwave spectroscopic study of the analogous H_2O−HCCH complex,[3] the height of the inversion barrier was determined to be sufficiently small that all vibrational levels were above this barrier, resulting in observation of an effective C_{2v} structure. A separate infrared and ab initio study on H_2O−HCCH[4,5] confirmed a very small barrier at the C_{2v} planar geometry, with the zero point level lying above this barrier. An ab initio calculation of the potential energy surface (PES) for the H_2O−HCCH complex[6] revealed that basis set superposition error (BSSE) correction has a significant effect on the ground-state PES features, and makes the C_{2v} structure the global minimum. Corrections for the zero point energy (ZPE) were found to further increase the stability of the C_{2v} structure for H_2O−HCCH.

The present study of the DME−HCCH complex extends our systematic investigations of complexes of DME with simple linear molecules such as CO_2,[7] OCS,[8] and CS_2.[9] Several weakly bound systems involving acetylene have been previously characterized, including the acetylene dimer[10] (which exhibits large amplitude interconversion tunneling motions of the subunits), oxirane-HCCH,[11] formaldehyde−HCCH,[12] and thiirane−HCCH.[13] The latter three systems are of particular interest since in these complexes the HCCH molecule does not form a linear C−H···X hydrogen bond to the proton acceptor (X), but rather the HCCH is found to be tilted such that a secondary interaction between the triple bond of the HCCH and the CH protons of the acceptor species is observed. Given the structural similarities between DME and oxirane, the question arises as to whether the HCCH will form a linear hydrogen bond, with the C≡C−H aligned along the lone pair direction of the DME, or whether a significant deviation from linearity will result because of a secondary interaction between the methyl group hydrogen atoms of DME and the triple bond of HCCH. There is also the possibility of significant internal motions of the subunits relative to one another, which would lead to spectral splittings analogous to those observed in the DME−HF,[1] DME−HCl,[2] and DME−CS_2[9] complexes.

It should be noted that the DME−HCCH complex was among the systems included in a matrix isolation infrared study of acetylene and substituted alkynes complexed with the oxygen bases DME, ethylene oxide, furan, and acetone.[14] Although no structural deductions were made for this complex, it is noteworthy that the 88 cm^{-1} observed red shift of the C−H stretch frequency in the DME−HCCH complex was the largest of the four complexes studied with acetylene, indicating the strongest binding.[14]

II. Experimental Section

The rotational spectra of five isotopomers of the DME−HCCH complex were measured by Fourier transform microwave

* Address correspondence to this author. E-mail: sapeebles@eiu.edu. Phone: (217) 581-2679 Fax: (217) 581-6613.

10.1021/jp0507593 CCC: $30.25
Published on Web 05/25/2005

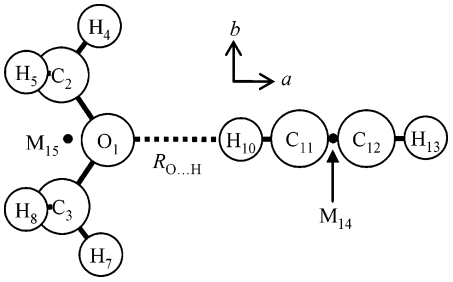

Figure 1. The C_{2v} structure showing the atom numbering and the single variable structural parameter ($R_{O\cdots H}$). M_{14} is the center of mass of the HCCH monomer, M_{15} is the center of mass of the DME. H_6 and H_9 are eclipsed by H_5 and H_8.

(FTMW) spectroscopy. The FTMW spectrometer has been described previously[15,16] and is based on the original Balle−Flygare design,[17] with numerous implementations and modifications from the University of Kiel.[18] DME (99.8%, Sigma-Aldrich) and HCCH (Gano Welding Co., Charleston, IL) were used to prepare samples that were about 1.5% in each component; these were diluted in "first-run" He/Ne (17.5% He, 82.5% Ne, BOC Gases) to a total backing pressure of 2.5 atm for optimum signal intensity. Samples were expanded into the evacuated Fabry−Perot cavity through the 0.8 mm orifice of a General Valve Series 9 nozzle at a repetition rate of 10 Hz. An initial search region of 6.5−8.3 GHz was scanned by using the autoscan facility of the spectrometer and numerous possible transitions were identified. This initial search region was based on ab initio predictions of the structure, which will be discussed in detail later.

Stark effect measurements were crucial in the assignment of the spectrum (see Section IIIA) and were carried out by the application of voltages up to ±5 kV to a pair of parallel steel mesh plates placed in the Fabry−Perot cavity, straddling the region of the molecular expansion. Electric field calibrations were carried out by daily measurement of the Stark shift of the $J = 1 \leftarrow 0$, $M = 0$ transition of the OCS molecule, using a dipole moment of 0.71521 D.[19]

The three ^{13}C singly substituted isotopic species were assigned in natural abundance (1.1% for substitutions on the acetylene molecule but 2.2% for the single substitution on the DME molecule due to the presence of a symmetry plane that makes the carbon atoms equivalent). To confirm the assignment of the ^{13}C-substituted acetylene isotopomers and to facilitate measurement of some of the less intense transitions, an isotopically enriched sample (99.2% $^{13}C_1$ acetylene, C/D/N Isotopes) was used to remeasure the spectra of the $^{13}C_{11}$- and $^{13}C_{12}$-substituted species (see Figure 1 for atom numbering). This enriched sample was prepared at slightly lower concentration (0.75% of each component in He/Ne) due to the small quantity of the isotope that was available, but the transition intensity was comparable to that of the normal isotopic species.

The rotational spectrum of the DME−DCCD isotopomer was measured by using a deuterated acetylene (DCCD) sample prepared by the action of 6 mL of D_2O on ca. 2 g of calcium carbide (Aldrich) in vacuo. The DCCD was condensed at liquid nitrogen temperature into a 1 L sample bulb. A 2-propanol/dry ice bath was placed between the reaction vessel and the sample bulb to trap water vapor. A sample of approximately 1.5% each in DME and DCCD was then prepared in the usual manner. Transitions for the DME−DCCD species were comparable in intensity to those of the normal isotopomer.

III. Results

A. Spectra. Spectral searches were based on ab initio calculations in which four possible structures were identified (Figure 2), including one C_{2v} geometry (structure **III**, with the HCCH aligned along the C_2 axis of DME, interacting via a C−H···O bond), and three C_s structures (structures **I**, **II**, and **IV**, again exhibiting C−H···O interactions and with the HCCH located in various positions in the plane that bisects the COC angle of the DME). More details on the ab initio calculations will be given in Section IV.

The initial assignment of the rotational spectrum for the DME−HCCH complex consisted of three very intense *a*-type transitions and was initiated by Stark effect experiments on the transition at 8252 MHz; the observed Stark shift was consistent with that predicted for a $J = 3_{13} \leftarrow 2_{12}$ transition for one of the ab initio structures. This line scaled accurately to both higher and lower J lines, so the $4_{14} \leftarrow 3_{13}$ and $2_{12} \leftarrow 1_{11}$ transitions were quickly located and the resulting rotational constants indicated that the complex was a near prolate top with Ray's asymmetry parameter, $\kappa \sim -0.95$. The most intense lines had signal-to-noise ratios in excess of 100 for 100 gas pulses, and a full width at half-maximum (fwhm) of about 40 kHz. Rigid rotor fits of the $K = 0$ and lower $K = 1$ transitions were of reasonably good quality, but the upper $K = 1$ lines were substantially displaced to low frequency by several tens of megahertz from the rigid rotor predictions. Attempts to assign unambiguously the $K \geq 2$ lines were unsuccessful due to the rapidly decreasing intensity of these transitions. Some candidates

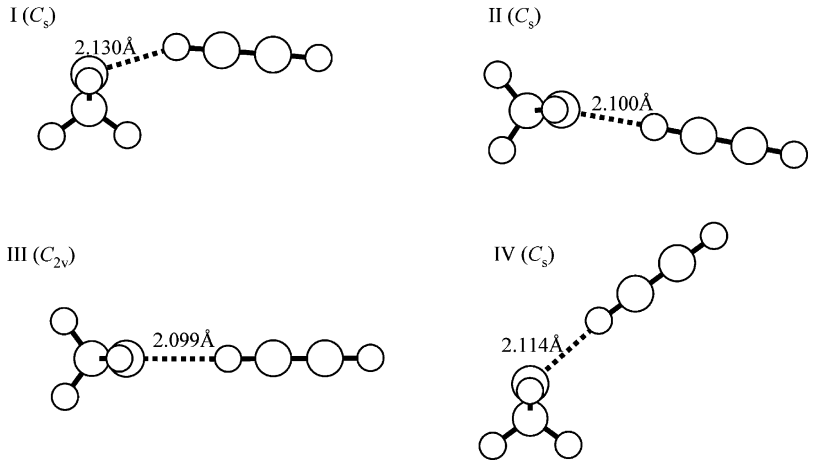

Figure 2. Structures **I**−**IV** obtained from the ab initio optimizations. The point group of each structure is given. Refer to Table 7 for interaction energies.

TABLE 1: Rotational Transition Frequencies for the Normal Isotopic Species of DME−HCCH

J'_{KaKc}	J''_{KaKc}	ν/MHz	$\Delta\nu$/MHz[a]
2_{12}	1_{11}	5502.3467	−0.0016
2_{02}	1_{01}	5725.0187	−0.0034
2_{11}	1_{10}	5916.6669	−0.0042
3_{13}	2_{12}	8252.3019	−0.0023
3_{03}	2_{02}	8579.2254	0.0037
3_{12}	2_{11}	8873.1857	−0.0007
4_{14}	3_{13}	11000.7912	0.0037
4_{04}	3_{03}	11423.3770	−0.0012
4_{13}	3_{12}	11827.4777	0.0061
5_{15}	4_{14}	13747.2867	−0.0001
5_{05}	4_{04}	14254.0814	0.0000
5_{14}	4_{13}	14778.6970	−0.0028
6_{16}	5_{15}	16491.2677	−0.0006

[a] $\Delta\nu = \nu_{obsd} - \nu_{calcd}$, where ν_{calcd} is computed from the spectroscopic constants in Table 2.

for $K = 2$ lines for the $J = 3 \leftarrow 2$, $4 \leftarrow 3$, and $5 \leftarrow 4$ transitions, as well as possible $K = 3$ lines for the $J = 4 \leftarrow 3$ transition, were observed in the predicted frequency regions, demonstrating the predictive ability of our fitted constants, but the observed transitions were messy, probably exhibiting small splittings, and their frequencies were not reproducible due to their low intensity. Whether the splitting of these higher K lines was due to internal motion of the methyl groups or to a small inversion splitting is not clear. Since the higher K lines were at the limit of detection of our spectrometer they were omitted from the spectral fit, and further attempts to measure them were abandoned.

The measured frequencies for the $K = 0$ and 1 transitions for the normal isotopic species of DME−HCCH are given in Table 1 and the spectroscopic parameters resulting from a fit to a Watson A reduction Hamiltonian[20] in the I^r representation with use of the SPFIT program of Pickett[21] are given in Table 2. Table 1 also lists the residuals from the last cycle of the least-squares fit. (Isotopic transition frequencies are available as Supporting Information.) It is apparent from the centrifugal distortion constants in Table 2 that the Hamiltonian does not entirely describe the interactions within this complex, the main concern being the negative sign of the Δ_J constant. Although rare, the phenomenon of a negative Δ_J has been observed occasionally, especially in cases where two tunneling states are assigned,[22] and it has been attributed to significant deviations from the semirigid rotor Hamiltonian (particularly when low-frequency van der Waals vibrational modes are present).[22] It should be noted that the magnitude of Δ_J is quite consistent throughout a range of different fits, although the sign does change depending on the particular set of constants being fitted. (Note that Δ_J does become positive if approximate frequencies for the $K > 1$ lines are included in the fit, albeit with an increased $\Delta\nu_{rms}$ value.) The constants fitted in Table 2 are those obtained after trials of several combinations of parameters; this was the minimum set of constants that we were able to fit and the set that showed the smallest correlations between parameters. Comparison of the constants for the different isotopes in Table 2 shows that the Δ_{JK} distortion constant consistently has a value of about 4.6−4.8 MHz. The large magnitude of Δ_{JK} is a further indication of the presence of large-amplitude vibrational motions, the effects of which are being absorbed by the distortion constants in our effective Hamiltonian. It should be pointed out that the values of the fitted constants are similar across the different isotopic species, helping confirm the consistency of our spectral assignment. Unfortunately, the small data set (only a-type transitions were observed) leads to a poor determination of the A rotational constant, and makes it difficult to fit more than the small set of parameters given in Table 2 without introducing significant correlation problems; observation of additional transitions for this complex in the millimeter wave region might allow additional distortion constants to be fitted, resolving the issues of the sign of Δ_J.

As mentioned above, the observed a-type $K = 0$ and 1 transitions were very intense, suggesting a significant μ_a component of dipole moment. No indication of any inversion doubling in the a-type lines was observed, in contrast to the spectra of the DME−CS_2 complex.[9] In that case, a motion of the CS_2 subunit from one side of the DME to the other caused inversion of the μ_c dipole component and led to observed splittings of 180 MHz in the c-type transitions and splittings of several tens of kilohertz for the a-type transitions. No candidates for c-type transitions were observed in the search region, as would be expected if the HCCH lies along a lone pair of the DME. It is acknowledged that given an inversion motion with a sufficiently low barrier, the c-type transitions could be split by a large enough amount that they would fall well outside our accessible spectral region. For instance, in the DME−HF complex,[1] a potential energy barrier of 0.71 kJ mol^{-1} to inversion of the HF molecule between the lone pairs of DME led to very large estimated c-type splittings of the order of 44 GHz and observed a-type splittings of between 30 and 120 MHz for transitions up to $J = 6 \leftarrow 6$; higher J a-type transitions measured in the millimeter wave region showed even larger splittings of up to several hundred megahertz. Conversely, a sufficiently low barrier would lead to all vibrational energy levels being above the barrier (as in the H_2O−HCCH complex[3]),

TABLE 2: Spectroscopic Constants for the Five Isotopomers of DME−HCCH[a]

parameter[b]	normal	$^{13}C_{11}$	$^{13}C_{12}$	$^{13}C_2$ (or $^{13}C_3$)	$^{2}H_{10,13}$
A/MHz	10382.5(17)	10373.6(12)	10380.1(13)	10117.6(16)	10350.4(14)
B/MHz	1535.7187(18)	1514.5348(17)	1486.0616(17)	1521.8391(23)	1448.3910(17)
C/MHz	1328.3990(17)	1312.4949(17)	1290.7486(17)	1312.7082(23)	1262.0408(17)
Δ_J/kHz	−12.355(18)	−11.699(17)	−11.004(17)	−12.93(2)	−10.210(17)
Δ_{JK}/MHz	4.7803(9)	4.6580(7)	4.5741(7)	4.8182(9)	4.4004(7)
δ_J/kHz	5.07(4)	4.90(4)	4.65(4)	5.20(8)	4.37(4)
ϕ_{JJ}/kHz	−0.0192(7)	−0.0190(7)	−0.0167(7)	−0.0183(15)	−0.0158(7)
N[c]	13	14	14	12	14
$\Delta\nu_{rms}$/kHz[d]	2.92	4.84	3.09	5.15	2.16
P_{aa}/u Å^2 [e]	330.425(4)	335.010(2)	341.466(3)	333.562(3)	350.272(3)
P_{bb}/u Å^2	50.018(4)	50.042(3)	50.074(3)	51.428(4)	50.174(3)
P_{cc}/u Å^2	−1.342(4)	−1.324(3)	−1.386(3)	−1.477(4)	−1.347(3)

[a] The singly substituted atom numbers refer to Figure 1. Uncertainties listed are the a priori errors obtained from the SPFIT program. [b] The smallest set of spectroscopic parameters fit that showed minimal correlations. The P^6 term (ϕ_{JJ}) is required for a satisfactory fit—exclusion of this parameter from the fit leads to an increase of the $\Delta\nu_{rms}$ value to 31 kHz. [c] N is the number of fitted transitions. [d] $\Delta\nu_{rms} = [\sum(\nu_{obsd} - \nu_{calcd})^2/N]^{1/2}$. [e] Second moments—see the text for discussion and definition.

TABLE 3: Calculated and Observed Stark Coefficients for Least-Squares Fits of μ_a for the DME−HCCH Dimer[a]

transition	$\|M\|$	$\Delta\nu/E^2$ (obsd)	$\Delta\nu/E^2$ (calcd)	% diff
$2_{11} \leftarrow 1_{10}$	0	3.5384	3.8526	−8.9
$3_{03} \leftarrow 2_{02}$	0	−0.7794	−0.8190	−5.1
	2	1.3976	1.5358	−9.9
$3_{13} \leftarrow 2_{12}$	0	−0.2099	−0.2389	−13.8
	1	3.4708	3.7649	−8.5
$3_{12} \leftarrow 2_{11}$	0	−0.2200	−0.2223	−1.0
	1	−3.4211	−3.4649	−1.3
	2	−13.399	−13.193	1.5

$$\mu_a = \mu_{\text{total}} = 1.91(10)\ \text{D}$$

[a] Stark coefficients are in units of 10^{-5} MHz V^{-2} cm^2.

in which case an effective C_{2v} structure would result and no *c*-type lines would be observed.

The majority of the transitions belonging to the DME−DCCD species showed no resolvable deuterium nuclear quadrupole hyperfine splitting and were not noticeably broadened relative to the undeuterated spectra. The $J = 2 \leftarrow 1$ transitions did show some splittings due to deuterium quadrupole coupling, although the splittings were not well resolved and attempts to assign this hyperfine structure were abandoned.

B. Dipole Moment. It was apparent early on that the μ_a dipole component was quite sizable and dominated the Stark shifts in the DME−HCCH complex. The experimental Stark coefficient data were fitted to a μ_a dipole component only. Attempts to fit a μ_c component gave very small values along with much larger uncertainties in the overall fit. The fitted value of μ_a is 1.91(10) D, with the results of the fit shown in Table 3. The poorer than usual fit is due to the combination of slow transitions (small $\Delta\nu/E^2$, which must be measured at high electric field to obtain reproducible shifts) and fast transitions (large $\Delta\nu/E^2$, which must be measured at low fields where the field calibration is unreliable). There are few transitions that have been measured over a wide enough range of field strengths to include both extremes. It should also be pointed out that care is needed in interpreting the lack of a μ_c dipole component: if the complex has C_{2v} symmetry then this component is zero by symmetry, whereas if the complex has effective C_{2v} symmetry (as we propose) then μ_c is averaged to zero due to inversion of the *c*-principal axis of the complex via the large amplitude motion.

Comparison of the fitted dipole moment for the DME−HCCH complex with the dipole moment of the DME monomer reveals a sizable enhancement of around 0.60 D relative to the dipole moment of 1.31 D for the monomer.[23] This will be discussed further in light of the ab initio results in Section IIID.

C. Structure and Bonding. The determination of an accurate structure of the DME−HCCH complex is frustrated by the measurement of only *a*-type rotational transitions. The large uncertainty therefore associated with the *A* rotational constant hinders many of the usual approaches to structure determination; however, second moment data are still useful in providing insight into the structure of this complex. Second moments are defined by expression 1; similar relationships exist for P_{bb} and P_{cc}.

$$P_{aa} = \sum_i m_i a_i^2 = 0.5(I_b + I_c - I_a) \qquad (1)$$

The location of the HCCH in the σ_v plane that bisects the COC angle of DME may be confirmed by inspection of the similar P_{bb} values for the five isotopic species (Table 2). With the exception of the $C_{2(3)}$ species (^{13}C substitution in the DME molecule), the P_{bb} values are all around 50.1(1) u Å^2, confirming that all but the $C_{2(3)}$ isotopic substitutions take place in the *ac* plane. The P_{bb} value of the $C_{2(3)}$ substituted isotopomer is some 1.4 u Å^2 above that of the ^{12}C-DME−HCCH species, consistent with the difference between the P_{aa} second moments of the ($^{12}CH_3$)$_2$O (P_{aa} = 47.04660(3) u Å^2) and (H$_3{}^{12}$C)O(^{13}CH$_3$) (P_{aa} = 48.38544(3) u Å^2) monomer species.[24] In addition, if the HCCH is located in the DME heavy atom plane, the P_{cc} value for the DME−HCCH dimer should be the same as that for the DME monomer (P_{cc} (DME) = 3.207326(3) u Å^2).[24] The magnitude of P_{cc} (1.35(4) u Å^2) is remarkably invariant (again with the exception of the $^{13}C_{2(3)}$ species), although the sign is negative. Although a negative value is unphysical based on the first definition of P_{cc} in eq 1, it is clear that if I_a is smaller than it should be structurally (for C_{2v} symmetry, I_a(dimer) should equal I_b(DME)), then the quantity P_{cc} will become negative. The closeness of the value of P_{cc} to that of the DME monomer seems sufficient evidence to indicate the HCCH lies in the *ab* plane.

Examination of the variation of the rotational constants across the isotopic species further corroborates the apparent existence of a C_2 symmetry axis. The *A* rotational constant is relatively invariant ($\leq$0.3%) except in the $^{13}C_{2(3)}$ substituted species where the isotopic substitution takes place off the *a*-axis. Note that the *A* rotational constant for the normal species is about 326 MHz above that of the *B* value for the DME monomer (*B*(DME) = 10056.509(6) MHz).[24] Likewise, the *A* rotational constant for the ^{13}C substitution of the DME molecule is 322 MHz above the *B* value for the (H$_3{}^{12}$C)O(^{13}CH$_3$) monomer (B = 9795.652-(5) MHz).[24] It is gratifying that these constants differ consistently from the monomer values; the differences can presumably be attributed to some vibrational contamination of the constants by the internal motions of the monomer subunits.

If C_{2v} symmetry is assumed for the DME−HCCH complex, and the DME[24] and HCCH[25] structures are assumed fixed at the literature values, only one structural parameter (the separation of the two monomers, $R_{O\cdots H}$) remains to be fitted. Structural determination of the DME−HCCH complex followed three different methods, namely, (a) a fit of the intermolecular separation to the quantity ($B + C$) for all isotopic species together and for the individual species, (b) a least-squares fit of isotopic moments of inertia to the intermolecular separation (again, either all isotopic data together or fitting each isotope separately), and (c) Kraitchman single isotopic substitution calculations of the principal axis coordinates of the substituted atoms.

For method a, a fit of all isotopic data using the STRFIT87 program of Schwendeman[26] gave a large standard deviation of around 1.5 u Å^2; this and all subsequent fits of individual isotopic data consistently gave an O···H separation of around 2.078 Å (Table 4).

The least-squares fits of method b utilized the STRFITQ program[26] and combinations of the I_a, I_b, and I_c moments for the different isotopic species were fitted. This method gave similar structural parameters as were obtained from the fits of ($B + C$) described above in method a (the average $R_{O\cdots H}$ for method b = 2.081 Å), although with much larger standard deviations ($\sim$4 u Å^2); this is a further indication of the contamination of the ground-state moments of inertia by the internal motions. Least-squares fits of the individual moments I_b and I_c for each isotopic species straddled the values obtained from the fit to the quantity ($B + C$). For instance, a least-squares fit of I_a, I_b, and I_c together for the normal isotopomer gives $R_{O\cdots H}$ = 2.082(20) Å, a fit of I_b only gives $R_{O\cdots H}$ = 2.054(2) Å, and a fit of I_c only gives $R_{O\cdots H}$ = 2.110(2) Å. Similar fits

TABLE 4: Results of the Least-Squares Fit of the $R_{O\cdots H}$ Distance to the Quantity ($B + C$) for the Various Isotopic Species of DME−HCCH

species fitted	$R_{O\cdots H}$/Å	R_{CM}[a]/Å
all five isotopomers	2.0780(7)[b]	4.2853(7)
Normal	2.080(2)	4.288(2)
DME−H^{13}C≡^{12}CH	2.079(2)	4.286(2)
DME−H^{12}C≡^{13}CH	2.078(2)	4.286(2)
^{13}C-DME−HC≡CH	2.077(2)	4.285(2)
DME−DC≡CD	2.076(2)	4.284(2)
average[c]	2.078(2)	4.286(2)
best[d]	2.08(3)	4.29(3)
ab initio[e]	2.099	4.307

[a] The center of mass separation (R_{CM}) is calculated from the fitted O···H distance assuming fixed literature monomer values. [b] ΔI_{rms} = 1.53 u Å^2 for this fit. Since for each of the other fits we are fitting one equation ($B + C$) to one parameter ($R_{O\cdots H}$) the ΔI_{rms} will be zero. [c] Average $R_{O\cdots H}$ and R_{CM} distances are calculated from the above fits. [d] Best guess structure taking into account the variation in $R_{O\cdots H}$ that is observed when fitting different combinations of the experimental data. [e] Ab initio structure from MP2/6-311++G(2d,2p) calculation (structure **III**; Figure 2).

TABLE 5: Principal Axis Coordinates for the DME−HCCH Dimer (in Å)[a]

substituted atom	*a*	*b*	*c*
$^{13}C_{11}$	−2.138	0.0000	0.008
	[2.153]	[0.159]	[0.134]
$^{13}C_{12}$	−3.342	0.000	0.005
	[3.340]	[0.243]	[0.000]
$^{13}C_2$ (or $^{13}C_3$)	1.797	±1.166	0.000
	[1.776]	[1.202]	[0.000]

[a] The inertial fit coordinates are taken from the fit of I_b and I_c moments of all isotopic species. Absolute values of Kraitchman coordinates are given in brackets for the singly substituted atoms. Uncertainties in Kraitchman coordinates are calculated to be ±0.001 Å or less.

for the other isotopic species gave consistent variations; hence, the uncertainty in the $R_{O\cdots H}$ distance given in the penultimate row of Table 4 is intended to reflect this variability. Although our fits give an average value of $R_{O\cdots H}$ of around 2.078(2) Å, we feel that, in light of the dependence of the intermolecular separation on the combination of moments of inertia included in the fit, a larger uncertainty of $R_{O\cdots H}$ = 2.08(3) Å, which encompasses the full range of values, is more realistic.

The determination of the principal axis coordinates obtained from the Kraitchman single isotopic substitution calculations[27] (method c) is also complicated by the poorly determined *A* rotational constant. The resulting principal axis coordinates are shown in Table 5, where they are compared with the principal axis coordinates from the least-squares fit of the moment of inertia data for all five isotopic species (method b). It can be seen that the coordinates are very similar, with the worst agreement (for nonzero coordinates) being shown by $^{13}C_{2(3)}$ (which also has the least well determined rotational constants). The *b*- and *c*-coordinates of substituted atoms C_{11} and C_{12} are slightly nonzero (presumably again due to vibrational contamination of the moments of inertia) but not sufficiently nonzero to seriously challenge the assumption of C_{2v} symmetry. Note that the C≡C distance in the acetylene molecule derived from the calculated Kraitchman coordinates is 1.198 Å, in excellent agreement with the literature value of 1.203 Å.[25] Furthermore, the distance between the methyl group carbon atoms of DME is computed to be 2.404 Å, compared to the literature value of 2.332 Å;[24] this agreement is much worse although still acceptable in light of the much poorer quality of the spectral fit for this species.

TABLE 6: Comparison of O···H Distances in Related Complexes

complex	$R_{O\cdots H}$/Å
$(CH_2)_2O$−HCCH[a]	2.40(2)
H_2C=O−HCCH[b]	2.39
H_2O−HCCH[c]	2.229
DME−HCCH[d]	2.08(3)
DME−HF[e]	1.642
DME−HCl[f]	1.766

[a] Oxirane−HCCH; ref 11. [b] Reference 12. [c] Reference 3. [d] This work. [e] This is an MP2 calculated value (ref 1) since insufficient isotopic data were available to fit this distance. However, given the quality of the agreement of the MP2 value with the partial r_0 fitted value from the DME−HCl complex (ref 2), it is reasonable to assume this distance is within 0.02 Å of the experimental distance. [f] Reference 2.

TABLE 7: The Interaction Energies (ΔE, in kJ mol^{-1}), Rotational Constants, and Dipole Moment Components of the Four ab Initio Structures (I−IV; Figure 2) Calculated for the DME−HCCH Complex at the MP2/6-311++G(2d,2p) Level[a]

	I	II	III	IV
(i) ΔE	−16.73	−16.51	−16.50	−16.46
(ii) ΔE (+ZPE)	−13.24	−13.52	−13.49	−13.38
(iii) ΔE (+ZPE+BSSE)	−9.62	−10.16	−10.15	−9.87
imaginary frequencies[b]		14*i*, 4*i*	14*i*	22*i*
A/MHz	8714	10012	10066	9383
B/MHz	1840	1502	1496	1608
C/MHz	1629	1330	1324	1427
μ_a/D	0.88	2.09	2.12	1.65
μ_c/D	1.41	0.27	0.00	0.99

[a] Interaction energies are given (i) uncorrected, (ii) ZPE corrected, and (iii) BSSE+ZPE corrected, as described in the text. [b] Values of imaginary frequencies (in cm^{-1}) are obtained from the vibrational frequencies calculated from an optimized structure on the BSSE uncorrected potential energy surface. The vibrational motions corresponding to the imaginary frequencies for each structure are described in the text.

The best guess $R_{O\cdots H}$ distance of 2.08(3) Å determined above is listed in Table 6 alongside O···H distances for several related acetylene complexes, with DME−HF[1] and DME−HCl[2] data included for comparison. It can be seen that the O···H distance determined for the DME−HCCH complex is the shortest of the values for the listed acetylene complexes. It is still, however, considerably longer than the values found in the DME complexes with HF[1] and HCl.[2] While this presumably indicates a relatively strong C−H···O bond in the DME−HCCH complex, the interaction is still considerably weaker than a conventional H-bond as observed in DME−HF or DME−HCl.

D. Ab Initio Calculations. Structure optimizations were carried out on the DME−HCCH complex up to the MP2 (frozen core)/6-311++G(2d,2p) level. The calculations were run with the Gaussian 98 suite of programs (G98W[28] on a desktop PC for the structure optimizations and G98[29] on a Tru64 Unix workstation for the vibrational frequency calculations). Four stationary points were identified on the potential energy surface with the interaction energies (Table 7) highlighting the flatness of the potential. These structures are pictured in Figure 2; they are related by a motion of the HCCH subunit around the DME in the σ_v plane that bisects the COC angle. (It should be stressed that some of these structures (structure **II** for instance) may be artifacts of the optimizations and might fail to be recognized as minima with higher level calculations; this will be addressed in more detail below). Two much higher energy minima on the PES (both involving interaction of the methyl group hydrogen atoms of DME with the triple bond of acetylene) were identified, but these structures were several hundred wavenumbers less

stable and so were not considered further, especially in light of the experimental isotopic spectral assignments. Table 7 lists three different computed interaction energies for the structures **I**−**IV**: (i) calculated without BSSE or ZPE corrections, (ii) calculated with ZPE corrections, and finally (iii) calculated including both BSSE and ZPE corrections. BSSE corrections were carried out according to the procedure of Xantheas,[30] and include small monomer relaxation contributions. The order of stability changes with the addition of ZPE corrections, with the previously most stable structure (**I**) becoming the least stable when ZPE corrections are considered. Incorporation of BSSE corrections maintained the new order of relative stabilities, but further increased the energy difference between the most and least stable geometry. Note that the difference between the two lowest energy structures at this level is very small (∼0.01 kJ mol^{-1}; Table 7). The final energy ordering (from most to least stable) is therefore **II**, **III**, **IV**, **I**. Table 7 also lists the number of imaginary frequencies obtained during the vibrational frequency calculation and all but structure **I** are found to have at least one imaginary frequency at the MP2/6-311++G(2d,2p) level. The hazards of optimizations of weakly bound floppy complexes at this level of theory are well illustrated in this case, where consideration of the effects of ZPE and BSSE on the energies has significant effects on both the energy ordering and vibrational frequencies.[31,32]

Structure **I** has C_s symmetry and the hydrogen atom of HCCH interacts with the oxygen atom of DME; this structure was the most stable before corrections for BSSE and ZPE were applied and was the only structure that was classified as a minimum according to the frequency calculations at this level. The hydrogen bond in this structure shows a reasonably large deviation from linearity (the O···H−C angle is ∼159°) since the HCCH is tilted toward the DME, perhaps hinting at a secondary interaction between the methyl group hydrogen atoms of the DME and the electron rich triple bond of the acetylene; however, the calculated distance between the nearest methyl group hydrogen atom and the triple bond is around 3.65 Å, considerably longer than might be expected for any significant C−H···π interaction. In contrast, in the oxirane−HCCH complex the distance from the closest hydrogen atoms of $(CH_2)_2O$ to the triple bond was found to be about 2.6 Å,[11] while the distance from the aldehyde proton to the triple bond in the formaldehyde−HCCH complex was about 2.8 Å.[12] Given the flatness of the PES for DME−HCCH, higher level ab initio optimizations with more stringent convergence criteria could yield additional insight into the possible C−H···π interactions that might stabilize structure **I**.

Structure **II** is also of C_s symmetry and lies very close in energy to the C_{2v} structure (**III**)—see Table 7. The HCCH subunit lies only slightly off the C_2 axis of the DME and presumably is identified as a minimum by the optimization procedure due to the very flat nature of the PES around the minima. The imaginary frequencies shown in Table 7 correspond to motions of the HCCH toward the C_{2v} structure and in a plane perpendicular to this.

Structure **III** differs little in geometry from structure **II** although it has C_{2v} symmetry, with the HCCH lying directly along the C_2 axis of DME. The C_{2v} structure **III** is the second most stable geometry when BSSE and ZPE corrections are applied, although less than 0.01 kJ mol^{-1} separates it from the most stable geometry (structure **II**). Interestingly, the MP2 computed dipole moment of structure **III** ($\mu_a = 2.12$ D) shows an enhancement of 0.69 D relative to the computed dipole moment of DME monomer optimized at the same level ($\mu_a =$ 1.43 D). This is comparable to the experimental dipole moment enhancement of 0.60 D. It should be noted that one imaginary frequency was calculated for this conformation; this vibrational mode corresponds to a tilt of the HCCH away from the C_2 axis of DME (with the HCCH remaining in the heavy atom plane of the DME).

Structure **IV** is of C_s symmetry with the HCCH aligned roughly along the direction of the lone pair of the oxygen atom. This structure is the least stable of the four structures on the uncorrected PES, although it is still only the third most stable when ZPE and BSSE corrections are applied. The single imaginary frequency shown in Table 7 for structure **IV** involves a motion of the HCCH toward the C_{2v} structure.

A more complete ab initio study might help to clarify the form of the PES for this weakly bound and floppy complex; however, these high-level studies are beyond the present scope of the work. The ab initio results presented here are intended only to highlight the small energy differences between the geometries and to assist in interpretation of the spectroscopic data. Ideally, optimization on a counterpoise (CP) corrected potential energy surface[31] would be carried out for complexes of this nature. Such an approach has been shown to significantly alter the stabilization energies as well as affect the vibrational frequencies and even the geometry.[31,32] The slow convergence of the CP-corrected optimization,[33] in addition to our need for only a rough estimate of the energy barriers separating different structures, makes the application of this technique in the present study too computationally expensive.

IV. Conclusions

The analysis of the moments of inertia obtained from measurement of the rotational spectra of five isotopomers of the DME−HCCH weakly bound dimer reveals a structure that has effective C_{2v} symmetry. Since we obtained a large magnitude for Δ_{JK} and it was necessary to include a P^6 centrifugal distortion term to reduce the residuals to an acceptable level, it appears that even at the low temperatures of the supersonic expansion used in this experiment, wide amplitude motion of the subunits within the complex contaminates the rotational constants.

Ab initio calculations (once corrected for ZPE and BSSE) predict the C_{2v} structure (**III**) as the next to lowest energy configuration although there is only a 0.01 kJ mol^{-1} difference between structure **III** and the lowest energy C_s geometry (structure **II**, where the HCCH is tilted only very slightly off the C_{2v} axis). The energy differences between the minimum energy structures are very small (with a difference of less than 0.54 kJ mol^{-1} separating the lowest and highest energy configurations) and hence seem to be consistent with the observation of an effective C_{2v} structure. In addition, motion of the HCCH molecule between the lone pairs of the DME (as was seen in the DME−HF[1] and DME−HCl[2] complexes) requires surmounting a barrier of only around 0.29 kJ mol^{-1}. Significantly higher level ab initio calculations are needed to fully explore the nature of the minima on the PES and to elucidate the relative energies as well as to quantify the effects of BSSE on the optimization process.

Acknowledgment is made to the Donors of the Petroleum Research Fund (PRF No. 39752-GB6), administered by the American Chemical Society, for support of this research. The authors thank Prof. Robert L. Kuczkowski for valuable comments upon an early draft of this work.

Supporting Information Available: Tables of measured transition frequencies for the four isotopic species. This material is available free of charge via the Internet at http://pubs.acs.org.

References and Notes

(1) Ottaviani, P.; Caminati, W.; Velino, B.; Blanco, S.; Lessarri, A.; López, J. C.; Alonso, J. *Chem. Phys. Chem.* **2004**, *5*, 336.
(2) Ottaviani, P.; Caminati, W.; Velino, B.; López, J. C. *Chem. Phys. Lett.* **2004**, *394*, 262.
(3) Peterson, K. I.; Klemperer, W. *J. Chem. Phys.* **1984**, *81*, 3842.
(4) Block, P. A.; Marshall, M. D.; Pedersen, L. G.; Miller, R. G. *J. Chem. Phys.* **1992**, *96*, 7321.
(5) Block, P. A.; Marshall, M. D.; Pedersen, L. G.; Miller, R. G. *J. Chem. Phys.* **1993**, *98*, 10107.
(6) Tzeli, D.; Mavridis, A.; Xantheas, S. S. *J. Chem. Phys.* **2000**, *112*, 6178.
(7) Newby, J. J.; Peebles, R. A.; Peebles, S. A. *J. Phys. Chem. A* **2004**, *108*, 11234.
(8) Newby, J. J.; Peebles, R. A.; Peebles, S. A. *J. Phys. Chem. A* **2004**, *108*, 7372.
(9) Peebles, S. A.; Peebles, R. A.; Newby, J. J.; Serafin, M. M. *Chem. Phys. Lett.* In press.
(10) Fraser, G. T.; Suenram, R. D.; Lovas, F. J.; Pine, A. S.; Hougen, J. T.; Lafferty, W. J.; Muenter, J. S. *J. Chem. Phys.* **1988**, *89*, 6028.
(11) Legon, A. C. *Chem. Phys. Lett*. **1995**, *247*, 24.
(12) Howard, N. W.; Legon, A. C. *J. Chem. Phys.* **1988**, *88*, 6793.
(13) Batten, R. C.; Cole, G. C.; Legon, A. C. *J. Chem. Phys.* **2003**, *119*, 7903.
(14) DeLaat, A. M.; Ault, B. S. *J. Am. Chem. Soc*. **1987**, *109*, 4232.
(15) Hillig, K. W.; Matos, J.; Scioly, A.; Kuczkowski, R. L. *Chem. Phys. Lett.* **1987**, *133*, 359.
(16) Newby, J. J.; Serafin, M. M.; Peebles, R. A.; Peebles, S. A. *Phys. Chem. Chem. Phys.* **2005**, *7*, 487.
(17) Balle, T. J.; Flygare, W. H. *Rev. Sci. Instrum.* **1981**, *52*, 33.
(18) Grabow, J.-U. Ph.D. Thesis, University of Kiel, 1992.
(19) Muenter, J. S. *J. Chem. Phys.* **1968**, *48*, 4544.
(20) Watson, J. K. G. *J. Chem. Phys.* **1969**, *46*, 1935.
(21) Pickett, H. M. *J. Mol. Spectrosc.* **1991**, *148*, 371.
(22) See for example: (a) Arunan, E.; Emilsson, T.; Gutowsky, H. S.; Fraser, G. T.; de Oliveira, G.; Dykstra, C. E. *J. Chem. Phys.* **2002**, *117*, 9766. (b) Heath, J. R.; Saykally, R. J. *J. Chem. Phys.* **1991**, *94*, 1724. (c) Chuang, C.; Gutowsky, H. S. *J. Chem. Phys.* **1991**, *94*, 86.
(23) Blukis, U.; Kasai, P. H.; Myers, R. J. *J. Chem. Phys.* **1963**, *38*, 2753.
(24) Niide, Y.; Hayashi, M. *J. Mol. Spectrosc*. **2003**, *220*, 65.
(25) Harmony, M. D.; Laurie, V. W.; Kuczkowski, R. L.; Schwendeman, R. H.; Ramsay, D. A.; Lovas, F. J.; Lafferty, W. J.; Maki, A. G. *J. Phys. Chem Ref. Data* **1979**, *8*, 619.
(26) Schwendeman, R. H. 1974, *Critical Evaluation of Chemical and Physical Structural Information*; Lide, D. R., Paul, M. A., Eds.; Washington, DC, National Academy of Sciences; the STRFIT87 and STRFITQ programs used are the University of Michigan modified versions of the original Schwendeman code.
(27) Kraitchman, J. *Am. J. Phys*. **1953**, *21*, 17.
(28) Frisch, M. J.; Trucks, G. W.; Schlegel, H. B.; Scuseria, G. E.; Robb, M. A.; Cheeseman, J. R.; Zakrzewski, V. G.; Montgomery, J. A., Jr.; Stratmann, R. E.; Burant, J. C.; Dapprich, S.; Millam, J. M.; Daniels, A. D.; Kudin, K. N.; Strain, M. C.; Farkas, O.; Tomasi, J.; Barone, V.; Cossi, M.; Cammi, R.; Mennucci, B.; Pomelli, C.; Adamo, C.; Clifford, S.; Ochterski, J.; Petersson, G. A.; Ayala, P. Y.; Cui, Q.; Morokuma, K.; Malick, D. K.; Rabuck, A. D.; Raghavachari, K.; Foresman, J. B.; Cioslowski, J.; Ortiz, J. V.; Stefanov, B. B.; Liu, G.; Liashenko, A.; Piskorz, P.; Komaromi, I.; Gomperts, R.; Martin, R. L.; Fox, D. J.; Keith, T.; Al-Laham, M. A.; Peng, C. Y.; Nanayakkara, A.; Gonzalez, C.; Challacombe, M.; Gill, P. M. W.; Johnson, B. G.; Chen, W.; Wong, M. W.; Andres, J. L.; Head-Gordon, M.; Replogle, E. S.; Pople, J. A. *Gaussian 98*, revision A.11; Gaussian, Inc.: Pittsburgh, PA, 1998.
(29) Frisch, M. J.; Trucks, G. W.; Schlegel, H. B.; Scuseria, G. E.; Robb, M. A.; Cheeseman, J. R.; Zakrzewski, V. G.; Montgomery, J. A., Jr.; Stratmann, R. E.; Burant, J. C.; Dapprich, S.; Millam, J. M.; Daniels, A. D.; Kudin, K. N.; Strain, M. C.; Farkas, O.; Tomasi, J.; Barone, V.; Cossi, M.; Cammi, R.; Mennucci, B.; Pomelli, C.; Adamo, C.; Clifford, S.; Ochterski, J.; Petersson, G. A.; Ayala, P. Y.; Cui, Q.; Morokuma, K.; Malick, D. K.; Rabuck, A. D.; Raghavachari, K.; Foresman, J. B.; Cioslowski, J.; Ortiz, J. V.; Stefanov, B. B.; Liu, G.; Liashenko, A.; Piskorz, P.; Komaromi, I.; Gomperts, R.; Martin, R. L.; Fox, D. J.; Keith, T.; Al-Laham, M. A.; Peng, C. Y.; Nanayakkara, A.; Gonzalez, C.; Challacombe, M.; Gill, P. M. W.; Johnson, B. G.; Chen, W.; Wong, M. W.; Andres, J. L.; Head-Gordon, M.; Replogle, E. S.; Pople, J. A. *Gaussian 98*, revision A.9; Gaussian, Inc.: Pittsburgh, PA, 1998.
(30) Xantheas, S. S. *J. Chem. Phys.* **1996**, *104*, 8821.
(31) Simon, S.; Duran, H.; Dannenberg, J. J. *J. Chem. Phys*. **1996**, *105*, 11024.
(32) Tzeli, D.; Mavridis, A.; Xantheas, S. S. *J. Phys. Chem. A* **2002**, *106*, 11327.
(33) Reimann, B.; Buchhold, K.; Vaupel, S.; Brutschy, B.; Havlas, Z.; Spirko, V.; Hobza, P. *J. Phys. Chem. A* **2001**, *105*, 5560.